HHS Public Access

Author manuscript

Analyst. Author manuscript; available in PMC 2014 November 21.

Published in final edited form as:

Analyst. 2013 November 21; 138(22): 6766–6773. doi:10.1039/c3an01235b.

Determination of Aerosol Oxidative Activity using Silver Nanoparticle Aggregation on Paper-Based Analytical Devices

Wijitar Dungchai[a], **Yupaporn Sameenoi**[b,d], **Orawon Chailapakul**[e], **John Volckens**[c], and **Charles S. Henry**[b,*]

[a]Department of Chemistry, Faculty of Science, King Mongkut's University of Technology Thonburi, Prachautid Road, Thungkru, Bangkok, 10140, Thailand [b]Department of Chemistry, Colorado State University, Fort Collins, Colorado, 80523-1872, United States [c]Department of Environmental and Radiological Health Sciences, Colorado State University, Fort Collins, Colorado, 80523-1872, United States [d]Department of Chemistry, Faculty of Science, Burapha University, Chonburi, 20131, Thailand [e]Department of Chemistry, Faculty of Science, Chulalongkorn University, 10330, Thailand

Abstract

Airborne particulate matter (PM) pollution significantly impacts human health, but the cellular mechanisms of PM-induced toxicity remain poorly understood. A leading hypothesis on the effects of inhaled PM involves the generation of cellular oxidative stress. To investigate PM-induced oxidative stress, analytical methods have been developed to study the chemical oxidation of dithiothreitol (DTT) in the presence of PM. Although DTT readily reacts with several forms of reactive oxygen species, this molecule is not endogenously produced in biological systems. Glutathione (GSH), on the other hand, is an endogenous antioxidant that is produced throughout the body and is directly involved in combating oxidative stress in the lungs and other tissues. We report here a new method for measuring aerosol oxidative activity that uses silver nanoparticle (AgNP) aggregation coupled to glutathione (GSH) oxidation in a paper-based analytical device. In this assay, the residual reduced GSH from the oxidation of reduced GSH to its disulfide induces the aggregation of AgNPs on a paper-based analytical device, which produces a reddish-brown product. Two methods for aerosol oxidative reactivity are presented: one based on change in color intensity using a traditional paper-based techniques and one based on the length of the color product formed using a distance-based device. These methods were validated against traditional spectroscopic assays for DTT and GSH that employ Elman's reagent. No significant difference was found between the levels measured by all three GSH methods (our two paper-based devices and the traditional method) at the 95% confidence level. PM reactivity towards GSH was less than towards DTT most likely due to the difference in the oxidation potential between the two molecules.

Keywords

particulate matter; exposure assessment; oxidative stress; PADs; aerosol sampling

Corresponding author: Prof. Dr. Charles S. Henry, Fax: +1-970-491-1801, Tel: +1-970-491-2852, chuck.henry@colostate.edu.

Introduction

Epidemiological studies have shown that human exposure to airborne particulate matter (PM) is associated with numerous health effects including diseases of the cardiovascular, respiratory, and immune systems [1–5]. Although a definitive mechanism of PM-induced toxicity remains elusive, it is generally agreed that PM induces oxidative stress (either directly or through induction of biological systems), causing systematic both inflammation and cellular dysfunction. Recently, both cell-based and cell-free systems have been used to investigate the capacity of PM to induce oxidative stress. Cell-based assays using fluorescence [6], chemiluminescence [7, 8], electron spin resonance [9], glutathione ratio [10, 11], lipid peroxidation, immunoassay and/or macrophage-based methods [12, 13] have shed important light into the mechanisms of PM-induced oxidative stress. However, these methods are expensive, complex, and difficult to use in the field. These assays also tend to require large amounts of PM (tens to hundreds of micrograms), which, in turn, requires long sampling and analysis times. Cell-free measurements of PM reactivity (oxidative load) typically use filter collection of PM and sample extraction prior to analysis. Traditionally, oxidative stress markers such as polyaromatic hydrocarbons (PAHs), quinones and transition metal have been measured using chromatography, electrophoresis, spectroscopy and mass spectrometry [14, 15]. More recently, a method for estimating total oxidative load using dithiotheitol (the so called DTT assay) has been demonstrated [16, 17]. The method has been convincingly shown to correlate with oxidative stress in vitro and thus, has been suggested as an appropriate surrogate when biological assays are not suitable. In the DTT assay, aqueous or solvent-based extracts of PM are mixed with DTT and allowed to react for a fixed period of time. The reaction is then quenched and Elman's reagent is added, reacting with the remaining reduced DTT to produce a yellow solution that absorbs light at 412 nm. The rate of DTT consumption measured in this way is directly proportional to the oxidative capacity of the PM sample. The DTT assay provides higher throughput than cell-based measurements, provided sufficient PM sample is available (10–100 μg of PM per test), but also requires laboratory-based equipment to operate.

Microfluidic paper-based analytical devices (μPADs) have gained interest for point-of- use diagnostics due to their low cost, ease of operation, and ability to function without external power supplies or supporting equipment [18–24]. Moreover, μPADs were recently introduced as an alternative for measuring oxidative load, providing a relatively simple method that requires less sample and reagent relative to traditional methods [25]. Unlike the traditional DTT assay, the μPAD method does not require a separate PM extraction step. Instead, a small punch taken from a filter sample of PM is spotted with DTT and allowed to react for a specified time (~20 min). The residual DTT present on filter punch is then eluted onto a μPAD that contains Elman's reagent (which reacts with remaining DTT). The intensity of the yellow color product is used to infer the DTT consumption rate. With the μPAD-based approach, the oxidative load of PM was measured in less than 30 min. The μPAD method also requires minimal reagent (1 μL) due to its small size (approximately 6.25 cm^2 per device). Finally, because the μPAD requires only 3 μg of PM mass, shorter air sampling times and/or collection at lower flow rates (i.e., for personal sampling) is possible, making the device particularly attractive for exposure and risk assessment.

Although previous examples of the DTT assay have used Elman's reagent, the method is less than ideal because the extinction coefficient of the yellow product is low (~10^4 M^{-1} cm^{-1}). In recent years, nanoparticles have been widely used for colorimetric assays due to higher extinction coefficients than common organic dyes. Gold nanoparticle (AuNP) and silver nanoparticle (AgNP)-based colorimetric sensors have been reported for measuring thiols such as homocysteine (Hcy) [26–28], glutathione (GSH) [26], and cysteine (Cys) [29–31] in biological samples. The use of AgNPs has gained popularity for colorimetric sensing because AgNPs are inexpensive and have higher extinction coefficients than AuNPs [32–34]. The change color intensity or/and color hue of AgNPs on paper-based devices can be visualized with the naked eye making them attractive for many applications [35, 36]. Here, we present the first use of AgNP for colorimetric sensing on μPAD for rapid, simple, and sensitive determination of PM oxidative load based upon aggregation of AgNP in the presence of residual GSH. GSH is more biologically relevant as a probe for PM oxidative load (than DTT) because GSH is an abundant endogenous antioxidant [37, 38]. We demonstrate here the ability of an AgNP-based μPAD assay to quantify aerosol oxidative load via the GSH consumption. The effect of reaction time was studied using 1,4-naphthoquinone (1,4-NQ) as a standard oxidant for GSH consumption. The versatility of the μPADs technique was demonstrated by measuring PM oxidative load using two different detection motifs: traditional colorimetric intensity analysis and a recently reported distance-based detection paradigm [39]. Distance-based detection eliminates the need for an external scanner or camera because the length of the colored region can be interpreted by the naked eye. Finally, our μPAD device was also validated against a conventional assay (UV-visible spectroscopy) using GSH instead DTT, and no significant difference was observed ($P < 0.05$, paired t-test) between the methods.

Experimental

Reagent and Materials

Glutathione, reduced 98%, rhodamine B (RB), and 1, 4-naphthoquinone were obtained from Sigma-Aldrich (St. Louis, MO). Dimethylsulfoxide (DMSO) was purchased from EMD Chemical Inc. (Gibbstown, NJ). Tris-hydrochloride (Tri-HCl) was obtained from Mallinckrodt Barker, Inc. (Phillipsburg, NJ). Whatman No. 1 qualitative grade filter paper was purchased from General Electric Company (Schenectady, New York, USA). All chemicals were used as received without further purification.

Preparation of AgNPs

A suspension of silver nanoparticles (AgNPs), obtained from the Sensor Research Unit at Department of Chemistry, Chulalongkorn University, Thailand, was synthesized using chemical reduction [40–42]. Sodium borohydride ($NaBH^4$) and methylcellulose solutions were used as the reducing agent and stabilizer, respectively. A 20 mM solution of $AgNO_3$ (10 mL) was combined with 10 mL freshly prepared methylcellulose solution and the mixture was stirred for 10 min in an ice bath. Then 0.1 M $NaBH_4$ (2 mL) was added dropwise with continuous stirring at 0°C to the mixture. After the complete addition of $NaBH_4$ yellow colored silver nanoparticles were obtained. The shapes and particle size distributions of the

AgNPs with nominal mean diameters of 10 nm were confirmed by transmission electron microscopy.

GSH quantification using AgNP aggregation

Suspensions of silver nanoparticles will aggregate in the presence of reduced GSH [43]. This aggregation results in a color shift of the AgNP suspension, moving from orange to reddish-brown. The amount of GSH present can be measured by color intensity or color length, depending on the type of μPAD used (described in more detail below). Color intensity is quantified using ImageJ software (national institutes of health, NIH) and the length of the colored region is quantified using the naked eye, respectively. All quantified color intensities were measured as a difference between the assay spot and a corresponding control spot. To generate a standard curve, varying levels of a standard oxidant species, 1, 4-naphthoquinone (1,4-NQ) and a fixed amount of GSH were pipetted sequentially onto filter paper and allowed to react for 20 min. The color product on the filter paper was then analyzed using the process described above. The relationship between the 1,4-NQ concentration and the GSH consumption was plotted and used as the standard curve of GSH consumption for real sample analysis.

Designs and procedure

The approaches used to measure GSH with a traditional μPAD or a distance-based μPAD are shown in Figures 1A and 1B, respectively. All μPADs were designed and drawn using standard vector-based drawing software (CorelDraw). A wax printer (Xerox Phaser 8860) was used to print wax on Whatman #1 filter paper following previously reported methods [44, 45]. The conventional μPAD consisted of three layers: a top layer for sample loading, a middle layer as a flow valve, and a bottom layer for detection (Figure 1A). Double-sided tape (Scotch ™) was used to hold various layers of the μPAD together. The middle (valve) layer consisted of a polymer film to provide a hydrophobic barrier that prevented sample from moving between layers until desired. This layer prevented sample leakage and also controlled overall reaction time. The top layer consisted of a 6 mm diameter opening for sample addition (i.e., placement of the filter punch) with two channels (2 mm width) leading to sample reaction regions (Figure 1A). Samples for oxidative load analyses consisted of 6 mm diameter punches that were cut from air sampling filters used to collect PM. With the middle layer in place, a PM-laden filter punch was placed over the sample addition region. Two 5 μL aliquots of H_2O were then added to the punch to extract the water soluble portion of the PM and elute it onto the two reaction zones. One zone was spotted with 5 μL of GSH while the other zone received no GSH (acting as a reference blank). After 20 min, the valve was opened by removing the middle layer and 20 μL of buffer was added to each reaction zone to elute the remaining GSH downwards to the bottom (detection) layer. The detection layer consists of two collection reservoirs (6 mm each; one sample, one reference) that received flow from layer one; each collection reservoir was also connected to four detection regions (each 4.3 mm in diameter) to allow for multiple measurements per sample. Prior to adding the sample punch, the detection spots were modified with a 0.5 μL aliquot containing 1,000 mg/L AgNPs and 16 μM RB solution. The residual GSH reacted with AgNPs in the detection layer and generated a reddish-brown color. Once dry, the detection reservoirs were imaged using a desktop scanner (Xerox

DocuMate 3220 Scanner, color photo setting, 600 dpi). Then, color intensity is quantified using ImageJ software (NIH). The overall device shown in Figure 1A measures 55×25 mm (Length×Width). With this approach, the oxidative load of PM was measured in less than 35 min.

The distance-based detection system consisted of a sample addition region (6 mm diameter) connected to a detection channel (3×60 mm). The detection channel was patterned with a series of horizontal baffles (0.3×2 mm, and spaced at 3 mm intervals) designed to reduce flow velocity and increase reaction time between GSH and AgNPs (Figure 1B) [46]. The detection channel was modified using a solution that had 1,000 mg/L AgNPs. For analysis, a filter punch (6 mm diameter) containing a PM sample was placed into a petri dish and allowed to react with a 5 μL drop of GSH for 20 min. The filter punch was then transferred to the sample addition region and the remaining GSH eluted into the detection channel with 20 μL of buffer. The residual GSH then flowed down the detection channel and reacted with AgNPs present along the flow path. Color develops along the flow path until all of the GSH is consumed. Quantification is achieved by measuring color length. This assay finished within 30 min.

Analysis of oxidative load of various aerosols

Sample collection—Two types of aerosol samples were collected for device validation: high-volume and low-volume filter samples. The high-volume samples were collected at fixed sites representing specific PM sources. The low-volume samples were collected using a miniature pump and filter-cassette assembly, carried by volunteers on different days. The high-loading aerosol samples were collected from three different sources: biomass burning, urban air, and second-hand cigarette smoke. Two biomass burning $PM_{2.5}$ samples (samples B1 and B2) from the combustion of vegetation commonly-burned in North American wildfires were collected using a Hi-volume filter sampler at the USDA Forest Service's Fire Science Laboratory in Missoula, Montana as part of the Third Fire Lab at Missoula Experiment study [47]. Three urban aerosol samples (C1-C3 samples) were collected on quartz filters over separate, integrated three-day sampling periods in Cleveland, OH during the winter of 2008 using a Thermo Anderson Hi-Volume Air Sampler (Windsor, NJ, USA). The quartz filters were pre-baked in an oven at 550 °C for 12 h and wrapped in aluminum foil before use. Additionally, two samples of second-hand tobacco smoke (S1 and S2 samples) were created in a 1.0 m^3 aerosol chamber and sampled onto 37 mm filters (Mixed Cellulose Ester Membrane, Millipore, Billerica, MA) at 10 L/min and 1 atm. After sampling, the filters were stored at −20 °C. These 'real-world' samples were used to demonstrate the technique and also served as the basis for comparing the paper-based methods with the traditional spectroscopic methods.

The low-volume samples were collected using a personal air sampler for PM_{10} (PM size ≤ 10 μm) on two separate days spent in Fort Collins, CO. A Teflon-coated glass-fiber filter (Pallflex® T40A60, 37 mm, Pall Corporation, Ann Arbor, MI) was used in conjunction with a personal aerosol sampler (Personal Environmental Monitors, 761-203A or 761-200A, SKC, Inc.). A small sampling pump (Omni-400, BGI Incorporated, Waltham, MA) was used to draw air through each sampler at 4 L min^{-1}. Volunteers carried the personal sampler in a

backpack over a 24 hrs period during two distinctly different events: (1) a restaurant sample collected across an 8 h work shift in a restaurant kitchen followed 16 h doing normal activities (mixture of indoor and outdoor exposure over 24 hrs) and (2) a sample collected across a 24 hrs period within a volunteer's home in Fort Collins (a relatively clean environment that was free from other combustion or cooking sources). All filters were weighed before and after sample collection with a microbalance (Mettler-Toledo, model MX5) to determine total mass loading. No additional sample preparation was required for these experiments.

Analysis and validation—To validate our devices with the traditional DTT and GSH assay using UV-visible spectrometer, the high-volume filter samples (B1-B2 and C1-C3) were extracted into de-ionized water. Briefly, two 25 mm diameter punches from each filter sample were extracted into 5 mL of de-ionized water in a Nalgene Amber High Density Polyethylene (HDPE) bottle using sonication with heat (70 ± 5 °C) for 75 min. The aerosol extract was filtered through a 0.2 μm PTFE membrane (Millipore, Billerica, MA, USA) to remove insoluble materials. The filtered extract was kept in the dark at 4 °C until analysis by conventional μPAD, distance-based μPAD or UV-visible spectrometer. For the UV-visible spectrometer, the extracted solution was reacted with DTT or GSH for 20 min. The detection of residual DTT or GSH using Elman's reagent was achieved using a UV-visible spectrometer at 412 nm (Thermo Spectronic, Genesys 10 UV) [48]. For both paper-based devices, 5 μL aliquots of sample extract and GSH were sequentially pipetted onto the filter paper and allowed to react for 20 min. To quantify GSH consumption, the filter paper was transferred to the μPAD (conventional or distance-based) containing AgNPs, and the residual GSH from the filter punch was eluted onto the μPAD with 20 μL of buffer. For field samples, sample punches were placed directly into paper devices without extraction. All remaining steps were carried out as described above for the comparison experiments.

Results and discussion

Two paper-based analytical devices were developed to measure PM oxidative load. Unlike prior efforts in this field, GSH was used as the reactive thiol because it is an endogenous antioxidant and, thus, more biologically relevant than dithiothreitol. In this assay, reduced GSH is oxidized to its disulfide in the presence of reactive species associated with PM. The remaining reduced GSH reacts with AgNPs (Figure 1C) to generate a colored product.

A conventional μPAD was designed that contained three layers to allow both sample analysis as well as blank subtraction from a single filter sample. The μPAD has four detection areas coated with AgNPs to improve the precision of each measurement. The resulting color product was captured using an office scanner and the color intensity was analyzed using ImageJ software. The alternative μPAD utilizes distance-based detection. The AgNPs were pipetted onto paper in 0.5 μL increments along the length of the detection channel. The residual GSH flowed along the channel by capillary action, and the GSH reacted with AgNPs giving a reddish-brown color product. Once all of the GSH has reacted, the color development stopped even as solution continued to flow along the channel. GSH quantification is achieved by measuring the length of the color along the channel using the naked eye.

Optimization of AgNP concentration

AgNPs are an alternative colorimetric reagent for determination of residual GSH because they have a high extinction coefficient (~10^{10} M^{-1} cm^{-1}) relative to many molecular dyes. The -SH group in aminothiol compounds such as homocysteine, cysteine, and GSH is known to react with the AgNP surface causing nanoparticle aggregation [43, 49]. This aggregation leads to significant shifting in the absorption spectrum with concomitant visible color changes from yellow/orange to reddish-brown. The relationship between GSH concentration and color intensity/length was measured first. For intensity measurements, a background correction was applied to all samples. To enhance the sensitivity, Rhodamine B (RB) was added to the AgNP solution, as this compound (as well as Rhodamine 6G) can affect the plasmon and molecular resonances of AgNPs [50, 51]. According to previous reports, RB attaches to the surface of AgNPs through carboxyl group and non-covalent interactions whereas Rhodamine 6G attaches to the surface via non-covalent interaction [52]. The AgNP surface modified with RB in Tri-HCl buffer shifted the absorption spectrum of the AgNPs because of the increased electrostatic repulsion between modified RB-AgNPs relative to AgNPs without RB. This phenomenon increased the change in color intensity upon addition of GSH. The effect of RB concentration on slope of GSH calibration was also measured. The maximum slope for a GSH calibration curve was found at 16 μM of RB and 1,000 mg/L of AgNPs as shown in Figure 2. Moreover, other anions in the aerosol sample or buffer including Cl^-, SO_4^{2-} and NO_3^- did not significantly change the color intensity (data not shown). Thus, a final concentration of 16 μM of RB and 1,000 mg/L of AgNPs was selected all further experiments using the conventional μPAD.

Analytical figures of merit

The intensity of the color product in the conventional μPAD was proportional to the GSH concentration over the range of 0 to 2.5 nmol (Intensity = 12.54*GSH + 0.51, R^2 = 0.99) as shown in Figure 3A using the optimized conditions. The relative standard deviation (RSD, *n* = 5) of GSH calibration slope was found to be 8.7%. Although this standard deviation is higher than commonly reported for the traditional absorbance method, it is in-line with other μPADs [53–55].

Aerosol oxidative activity was next measured using the distance-based μPAD. With distance-based detection, no background correction was needed because a distinct color change can be seen visually. The detection channel was coated with only 1,000 mg/L of AgNP. A plot of sample reaction length as a Log function of the analyte concentration is shown in Figure 3B. Reaction length was log-linear in the range of 0.12 to 2 nmol GSH (Distance = 6.4*log-GSH + 7.5, R^2 = 0.99) and the RSD of GSH calibration slope was 5.1% (*n* = 5). The improvement in reproducibility for the distance-based μPAD relative to the traditional μPAD is most likely the result of the improved ability to distinguish the end point of the distance-based detection relative to the intensity change of the traditional device.

Performance of aerosol oxidative activity measurement

The effect of reaction time on GSH consumption rate was studied using 1,4-NQ as a model oxidant in the range of 0 to 15 ng 1,4-NQ with 2.5 nmol of initial GSH. The sensitivity of the assay demonstrated a significant improvement with increasing reaction time from 15 min

(slope = 0.037) to 20 min (slope = 0.062). No further improvement in slope was found at 25 min (slope = 0.066) as shown in Figure 4. As a result, 20 min was selected as the optimal reaction time. The impact of starting GSH amount on detection limit and working range was measured next. The detection limit (Table 1) was estimated as the concentration that produced a signal at 3 times greater than the standard deviation of a blank (n = 10). The working range was taken as the linear range between the intensity or distance and 1,4-NQ amount (Table 1). The lowest detection limit of 1,4-NQ was obtained at low starting GSH (0.5 nmol) but the largest working range was found at higher initial GSH. Meanwhile, the distance-based μPAD gave both the lowest detection limit and the widest working range at high initial GSH (1.25 nmol). Sensitivity is increased for high initial GSH concentrations because the length of the colored region is longer than at lower GSH concentrations. As a result, it was easier to distinguish changes in color at high initial GSH by the eye in the presence of smaller amounts of 1,4-NQ. These results show that the devices can be used for a variety range of aerosol oxidative reactivities in the field by tuning the initial amount of GSH on paper devices. For the low oxidative load of our samples, 0.5 nmol and 1.25 nmol of GSH were used to obtain the lowest detection limit for μPAD and distance-based detection, respectively.

Analytical applications

To validate the devices for aerosol oxidative activity determination with real samples, results for the traditional assay using either DTT or GSH with Elman's reagent were compared to the colorimetric and distanced-based μPADs. Five different samples of aerosol extracts (Figure 5A) were analyzed using all four methods. The DTT consumption rate measured by the traditional assay in all five samples (black bar in Figure 5A) was higher than the GSH consumption rate (red bar in Figure 5A) according to the stronger reducing power of DTT relative to GSH [56]. The GSH consumption rate measured by all three methods (colorimetric and distance-based μPAD and traditional Elman's reagent assay) was compared using analysis of variance (ANOVA, single factor) and plotted for correlation. No significant difference between the three methods was obtained at the 95% confidence level (*p-value* = 0.98). A good correlation between the traditional GSH assay and both μPAD devices was obtained with R^2 = 0.98 and 0.99 for μPAD and distance-based detection, respectively.

To further demonstrate the utility of our devices for real samples, four filter samples (S1–S2, ambient aerosols around Fort Collins and in the restaurant) were analyzed using the μPAD methods. The results shown in Figure 5B show a strong correlation between the traditional and distance-based μPAD methods (R^2 = 0.99); both devices could distinguish the high and low oxidative activity between cigarette smoke and ambient aerosols, respectively. Both μPAD devices can also be applied to filter samples collected in the field. The advantages of the traditional μPAD over distance-based μPAD include lower detection limit of 1,4-NQ and wider working range. However, the distance-based μPAD eliminates the need for an external scanner or camera. The analysis time of both our devices without any sample extraction was also less than 35 min, which marks a significant improvement over traditional spectroscopic assays (2 hrs)[14].

Conclusion

We demonstrate here the development of an AgNP colorimetric sensing method for aerosol oxidative activity using paper-based analytical devices. The determination of aerosol oxidative activity on paper devices was previously based on the use of Elman's reagent with DTT. Here, the reddish-brown color intensity and distance produced from the aggregation of AgNPs by GSH was used to estimate aerosol reactivity. The reddish-brown color intensity on μPAD provided a low detection limit for aerosol oxidative activity relative to previously reported methods. With distance-based detection, the length of reddish-brown color product can be readily discriminated by the naked eye. No significant differences for the aerosol oxidative activity measurement in filter samples between using our devices and the traditional GSH assay were observed. Both the distance-based detection and μPAD represent a highly sensitive, rapid and simple technique that should be applicable to personal exposure monitoring.

Acknowledgements

WD gratefully acknowledges the financial support from Chemistry department, Science Faculty, King Mongkut's University of Technology Thonburi and the Thailand Research Fund (MRG5580234). This work was supported by grants from the National Institute for Occupational Safety and Health (OH010050) and the National Institute of Environmental Health Sciences (ES019264).

References

1. Prahalad AK, Inmon J, Dailey LA, Madden MC, Ghio AJ, Gallagher JE. Chem. Res. Toxicol. 2001; 14:879–887. [PubMed: 11453735]
2. Pope CA 3rd, Bates DV, Raizenne ME. Environ. Health Persp. 1995; 103:472–480.
3. Sun QH, Hong XR, Wold LE. Circulation. 2010; 121:2755–2765. [PubMed: 20585020]
4. Crapo J, Miller FJ, Mossman B, Pryor WA, Kiley JP. Am. Rev. Respir. Dis. 1992; 145:1506–1512. [PubMed: 1596028]
5. Spira-Cohen A, Chen LC, Kendall M, Lall R, Thurston GD. Environ. Health Persp. 2011; 119:559–565.
6. Sauvain JJ, Setyan A, Wild P, Tacchini P, Lagger G, Storti F, Deslarzes S, Guillemin M, Rossi MJ, Riediker M. J. Occup. Med. Toxicol. 2011; 6(18):1–13. [PubMed: 21208428]
7. Boveris A, Cadenas E, Reiter R, Filipkowski M, Nakase Y, Chance B. Proc. Natl. Acad. Sci. U.S.A. 1980; 77:347–351. [PubMed: 6928628]
8. Ghio AJ, Meng ZH, Hatch GE, Costa DL. Inhal. Toxicol. 1997; 9:255–271.
9. Kadiiska MB, Mason RP, Dreher KL, Costa DL, Ghio AJ. Chem. Res. Toxicol. 1997; 10:1104–1108. [PubMed: 9348432]
10. Tietze F. Anal. Biochem. 1969; 27:502–522. [PubMed: 4388022]
11. Xiao GG, Wang MY, Li N, Loo JA, Nel AE. J. Biol.Chem. 2003; 278:50781–50790. [PubMed: 14522998]
12. Tamarit J, Cabiscol E, Ros J. J. Biol. Chem. 1998; 273:3027–3032. [PubMed: 9446617]
13. Shacter E, Williams JA, Lim M, Levine RL. Free Radic. Biol. Med. 1994; 17:429–437. [PubMed: 7835749]
14. Jung H, Guo B, Anastasio C, Kennedy IM. Atmos. Environ. 2006; 40:1043–1052.
15. Vidrio E, Phuah CH, Dillner AM, Anastasio C. Environ. Sci. Technol. 2009; 43:922–927. [PubMed: 19245037]
16. Sameenoi Y, Koehler K, Shapiro J, Boonsong K, Sun Y, Collett J, Volckens J, Henry CS. J. Am. Chem. Soc. 2012; 134:10562–10568. [PubMed: 22651886]
17. Li Q, Wyatt A, Kamens RM. Atmos. Environ. 2009; 43:1037–1042.

18. Jokerst JC, Adkins JA, Bisha B, Mentele MM, Goodridge LD, Henry CS. Anal. Chem. 2012; 84:2900–2907. [PubMed: 22320200]
19. Mentele MM, Cunningham J, Koehler K, Volckens J, Henry CS. Anal. Chem. 2012; 84:4474–4480. [PubMed: 22489881]
20. Dungchai W, Chailapakul O, Henry CS. Anal. Chem. 2009; 81:5821–5826. [PubMed: 19485415]
21. Martinez AW, Phillips ST, Wiley BJ, Gupta M, Whitesides GM. Lab Chip. 2008; 8:2146–2150. [PubMed: 19023478]
22. Martinez AW, Phillips ST, Whitesides GM, Carrilho E. Anal. Chem. 2010; 82:3–10. [PubMed: 20000334]
23. Cheng CM, Martinez AW, Gong JL, Mace CR, Phillips ST, Carrilho E, Mirica KA, Whitesides GM. Angew. Chem. Int. Ed. 2010; 49:4771–4774.
24. Yang XX, Forouzan O, Brown TP, Shevkoplyas SS. Lab Chip. 2012; 12:274–280. [PubMed: 22094609]
25. Sameenoi Y, Panymeesamer P, Supalakorn N, Koehler K, Chailapakul O, Henry CS, Volckens J. Environ. Sci. Technol. 2013; 47:932–940. [PubMed: 23227907]
26. Hepel, M.; Stobiecka, M. Fine Particles in Medicine and Pharmacy. Matijević, E., editor. Springer US; 2012. p. 241-281.
27. Lim IIS, Ip W, Crew E, Njoki PN, Mott D, Zhong C-J, Pan Y, Zhou S. Langmuir. 2006; 23:826–833. [PubMed: 17209640]
28. Leesutthiphonchai W, Dungchai W, Siangproh W, Ngamrojnavanich N, Chailapakul O. Talanta. 2011; 85:870–876. [PubMed: 21726712]
29. Li ZP, Duan XR, Liu CH, Du BA. Anal. Biochem. 2006; 351:18–25. [PubMed: 16500604]
30. Wei X, Qi L, Tan J, Liu R, Wang F. Anal. Chim. Acta. 2010; 671:80–84. [PubMed: 20541646]
31. Chen Z, Luo S, Liu C, Cai Q. Anal. Bioanal. Chem. 2009; 395:489–494. [PubMed: 19641904]
32. Stokes RJ, Macaskill A, Johan Lundahl P, Ewen Smith W, Faulds K, Graham D. Small. 2007; 3:1593–1601. [PubMed: 17647254]
33. Shrivas K, Wu HF. Rapid. Commun. Mass. Sp. 2008; 22:2863–2872.
34. Li H, Cui Z, Han C. Senor. Actuat. B-Chem. 2009; 143:87–92.
35. Apilux A, Siangproh W, Praphairaksit N, Chailapakul O. Talanta. 2012; 97:388–394. [PubMed: 22841097]
36. Ratnarathorn N, Chailapakul O, Henry CS, Dungchai W. Talanta. 2012; 99:552–557. [PubMed: 22967593]
37. Scibior D, Skrzycki M, Podsiad M, Czeczot H. Clin. Biochem. 2008; 41:852–858. [PubMed: 18394427]
38. Banne AF, Amiri A, Pero RW. J. Anti-Aging. Med. 2003; 6:327–334. [PubMed: 15142434]
39. Cate DM, Dungchai W, Cunningham JC, Volckens J, Henry CS. Lab Chip. 2013; 13:2397–2404. [PubMed: 23657627]
40. Leesutthiphonchai W, Dungchai W, Siangproh W, Ngamrojnavanich N, Chailapakul O. Talanta. 2011; 85:870–876. [PubMed: 21726712]
41. Bhui DK, Misra A. Carbohyd. Polym. 2012; 89:830–835.
42. Sarkar P, Bhui DK, Bar H, Sahoo GP, Samanta S, Pyne S, Misra A. Nanoscale. Res. Lett. 2010; 5:1611–1618. [PubMed: 21076672]
43. Stobiecka M, Coopersmith K, Hepel M. J. Colloid. Interf. Sci. 2010; 350:168–177.
44. Carrilho E, Martinez AW, Whitesides GM. Anal. Chem. 2009; 81:7091–7095. [PubMed: 20337388]
45. Zhong ZW, Wang ZP, Huang GXD. Microsyst. Technol. 2012; 18:649–659.
46. Apilux A, Ukita Y, Chikae M, Chailapakul O, Takamura Y. Lab Chip. 2013; 13:126–135. [PubMed: 23165591]
47. Hennigan CJ, Miracolo MA, Engelhart GJ, May AA, Presto AA, Lee T, Sullivan AP, McMeeking GR, Coe H, Wold CE, Hao WM, Gilman JB, Kuster WC, de Gouw J, Schichtel BA, Collett JL, Kreidenweis SM, Robinson AL. Atmos. Chem. Phys. 2011; 11:7669–7686.
48. S edlak J, Lindsay RH. Anal. Biochem. 1968; 25:192–205. [PubMed: 4973948]

49. Li HB, Cui ZM, Han CP. Sensor. Actuat. B-Chem. 2009; 143:87–92.
50. Zhao J, Jensen L, Sung JH, Zou SL, Schatz GC, Van Duyne RP. J. Am. Chem. Soc. 2007; 129:7647–7656. [PubMed: 17521187]
51. Kruszewski S, Cyrankiewicz M. Acta. Phys. Pol. A. 2012; 121:A68–A74.
52. Cui ZM, Han CP, Li HB. Analyst. 2011; 136:1351–1356. [PubMed: 21305084]
53. Mentele MM, Cunningham J, Koehler K, Volckens J, Henry CS. Anal. Chem. 2012; 84:4474–4480. [PubMed: 22489881]
54. Martinez AW, Phillips ST, Whitesides GM, Carrilho E. Anal. Chem. 2010; 82:3–10. [PubMed: 20000334]
55. Martinez AW, Phillips ST, Butte MJ, Whitesides GM. Angew. Chem. Int. Ed. Engl. 2007; 46:1318–1320. [PubMed: 17211899]
56. Johnston PA, Soares KM, Shinde SN, Foster CA, Shun TY, Takyi HK, Wipf P, Lazo JS. Assay. Drug. Dev. Techn. 2008; 6:505–518.

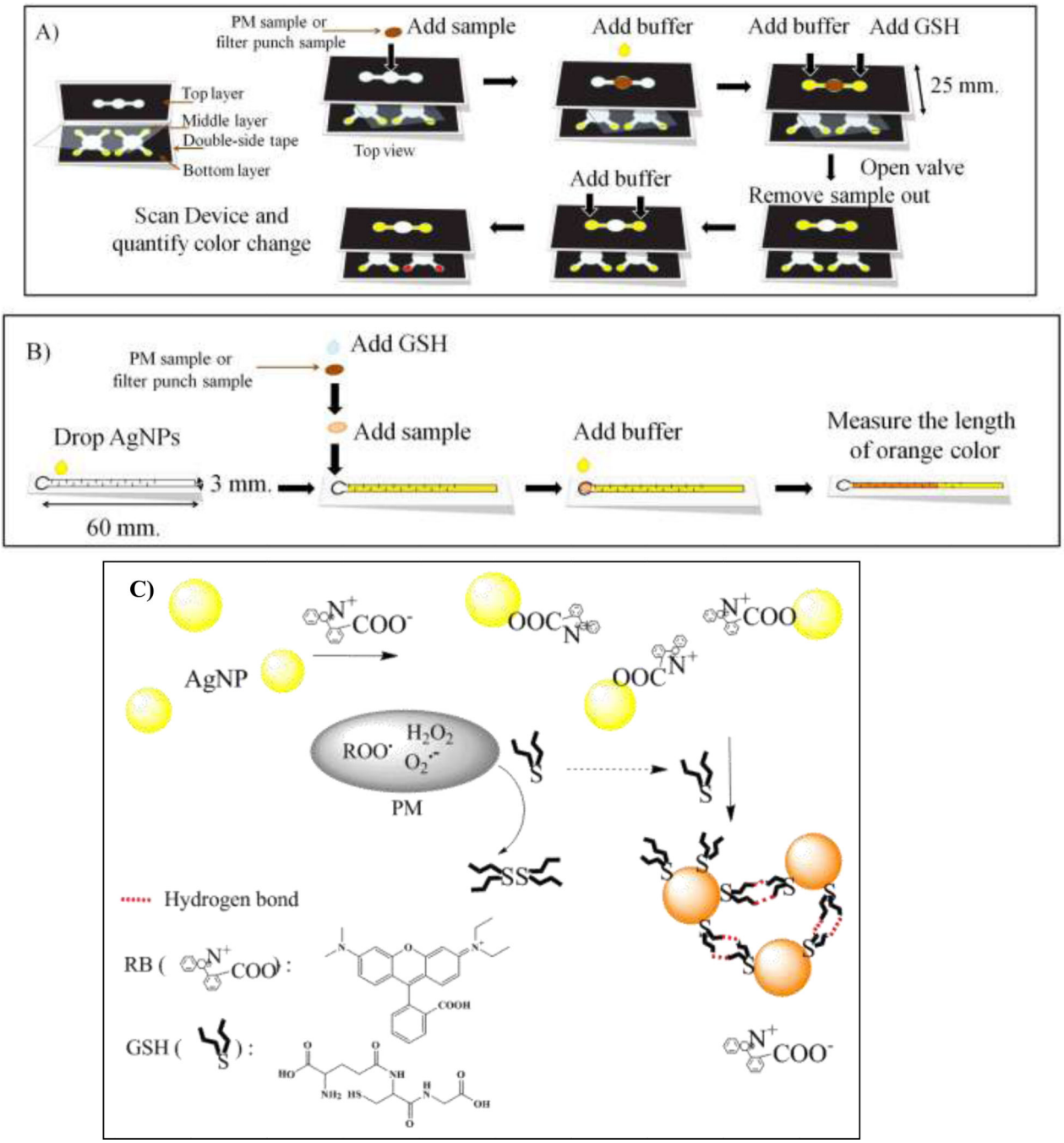

Figure 1.

Schematic drawings of the device designs and general analytical methods of (A) a traditional μPAD and (B) a distance-based μPAD for the determination of the aerosol oxidative load. (C) Schematic diagram of the AgNP aggregation mechanism for determination of residual GSH.

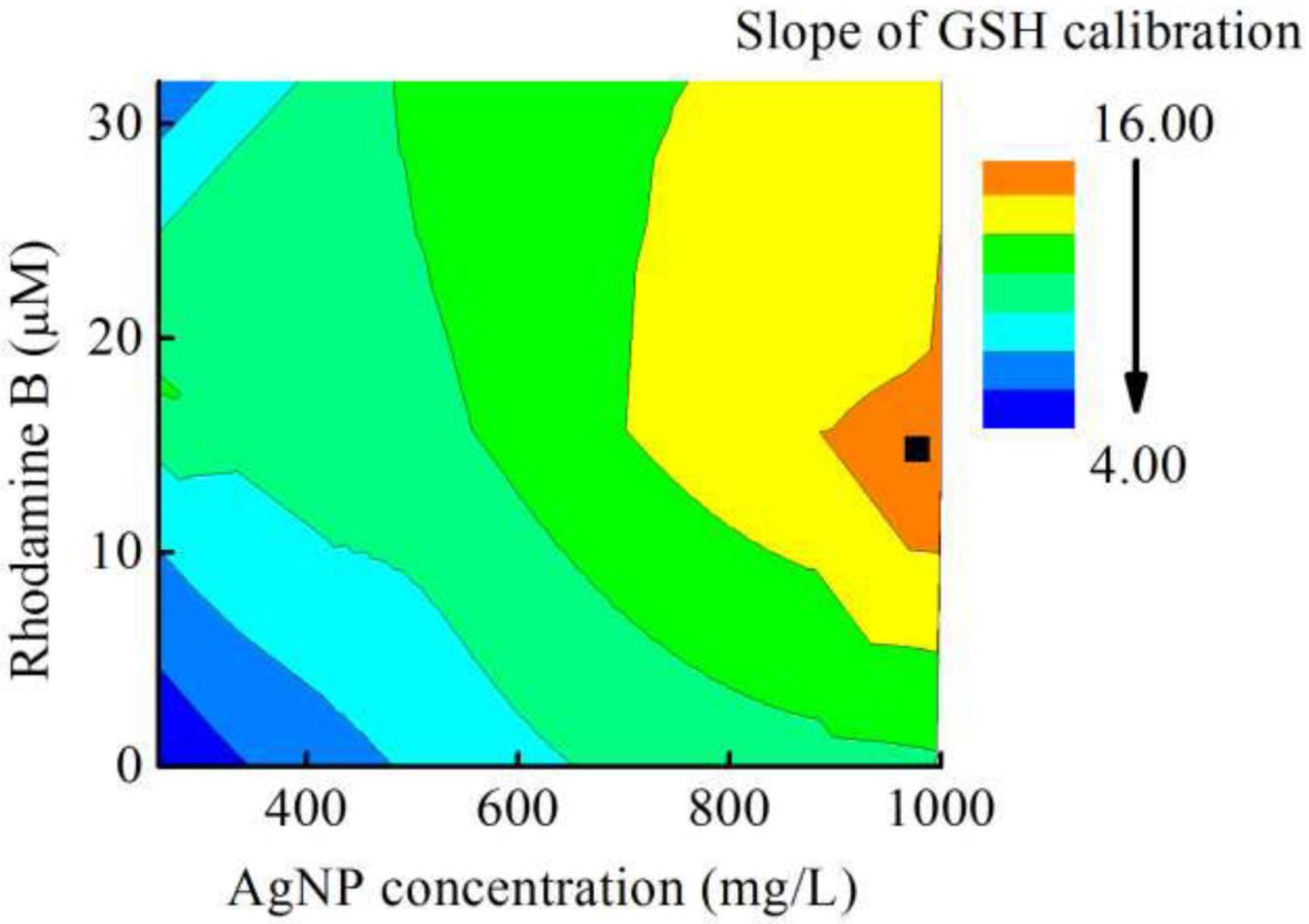

Figure 2.

Optimization of RB and AgNP concentrations on the two different types of μPADs. The optimized condition represented by ■ in this figure.

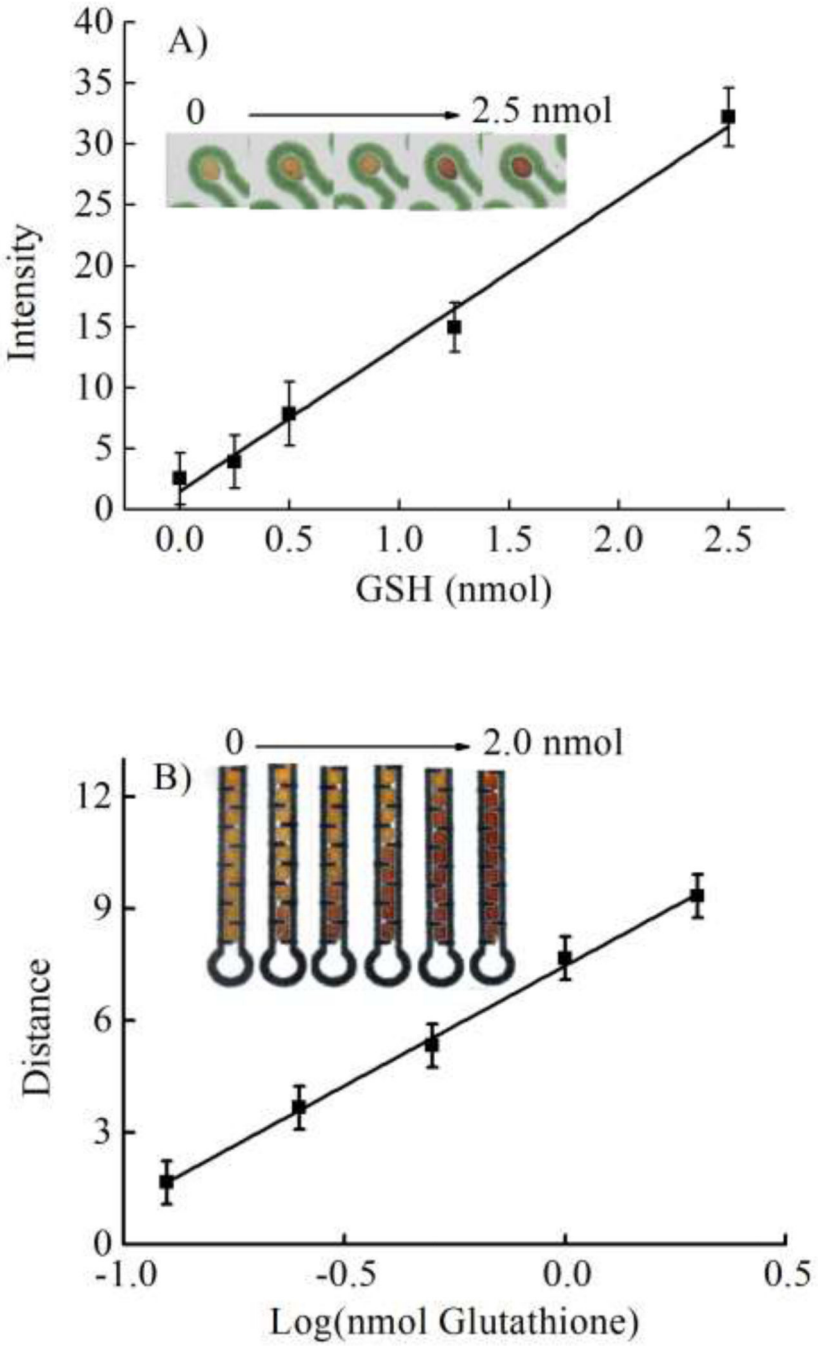

Figure 3.
(A) Calibration of GSH using the μPADs. (B) Calibration of GSH using the distance-based μPAD, *n* = 3.

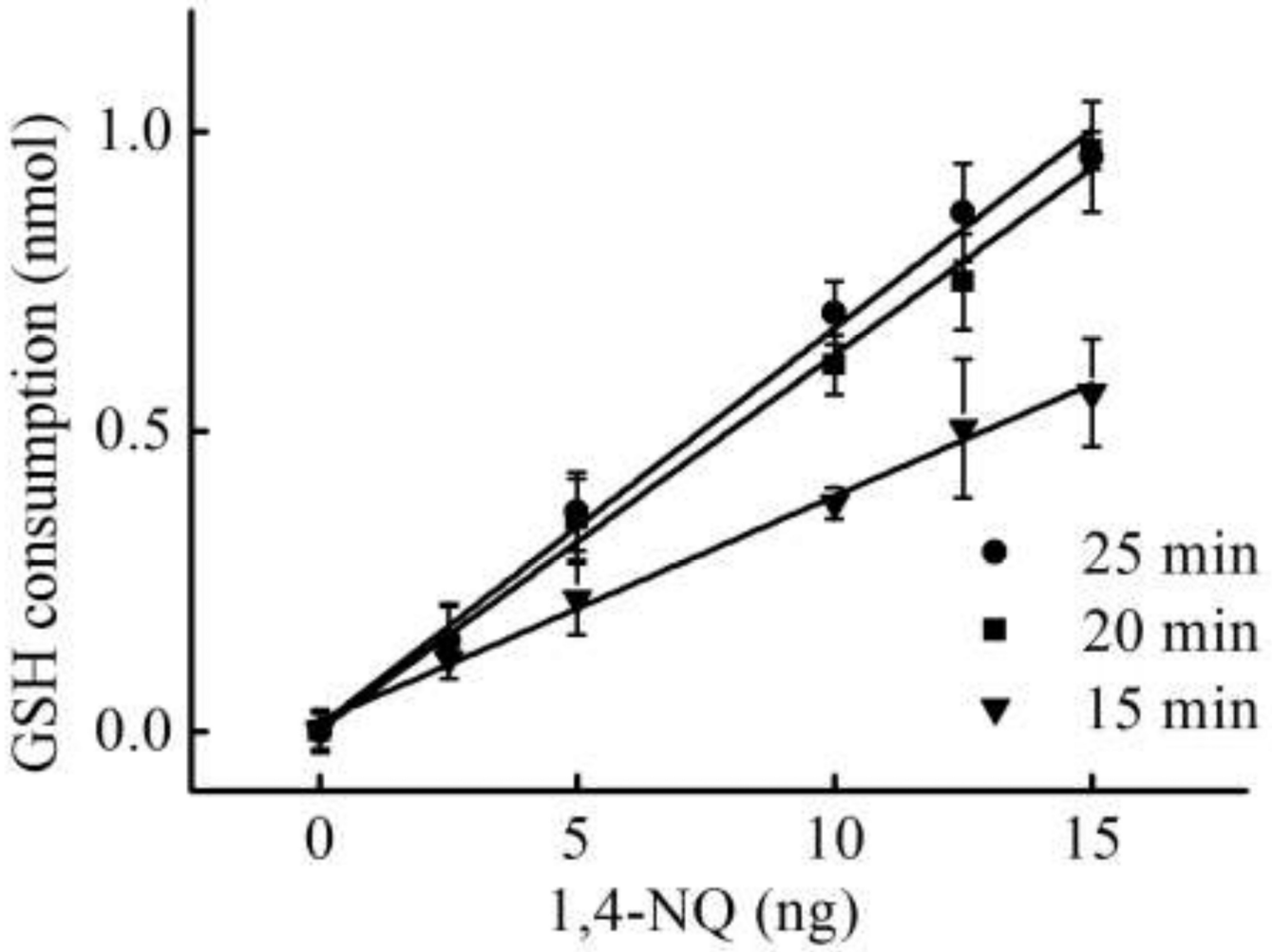

Figure 4.
Optimization of reaction time between GSH and 1,4-NQ at 2.5 nmol of the initial GSH, *n* = 3.

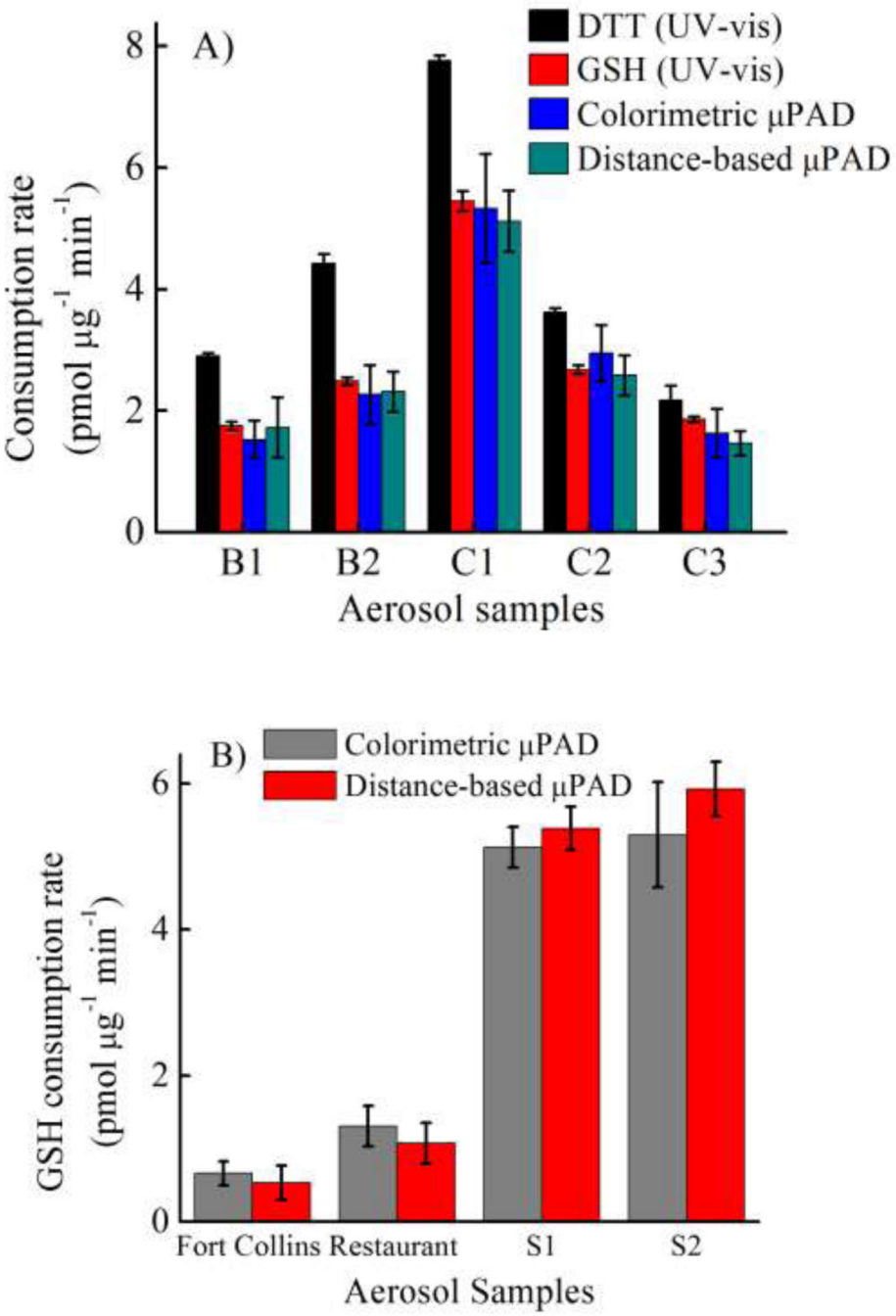

Figure 5.
Method validation using (A) an extracted sample and (B) a filter sample, $n = 3$.

Table 1

Linearity and LOD of 1,4-NQ in the presence of various initial GSH amount with 20 min of reaction time.

Devices	GSH (nmol)	LOD of 1,4-NQ (ng)	Linearity of 1,4-NQ (ng)
μPADs	2.5	11.0	0 – 75
	1.25	6.5	0 – 35
	0.5	3.7	0 – 25
Distance-based μPAD	1.25	10.0	5–25
	0.5	20.0	15–30